

Carbon-to-chlorophyll ratio and carbon content of phytoplankton community at the surface in coastal waters adjacent to the Zhujiang River Estuary during summer

Xiaoyong Yu^{1,2}, Jie Xu^{1,2*}, Aimin Long^{1,2}, Ruihuan Li¹, Zhen Shi¹, Qian P Li^{1,2}

¹ State Key Laboratory of Tropical Oceanography, South China Sea Institute of Oceanography, Chinese Academy of Sciences, Guangzhou 510301, China

² University of Chinese Academy of Sciences, Beijing 100049, China

Received 11 April 2018; accepted 18 May 2018

© Chinese Society for Oceanography and Springer-Verlag GmbH Germany, part of Springer Nature 2020

Abstract

Chlorophyll *a* (Chl *a*), particulate organic carbon (POC) and biogenic silica (BSi) were determined in coastal waters adjacent to the Zhujiang (Pearl) River Estuary (ZRE) during summer, in order to examine the C:Chl *a* ratio of phytoplankton and phytoplankton carbon in the plume-impacted coastal waters during summer, as well as to assess the relative contribution of diatoms to the phytoplankton biomass, by the regression between Chl *a*, POC and BSi. Our results showed that the C:Chl *a* ratio (g/g) of phytoplankton was high (up to 142), likely due to high light intensity and nutrient limitation. The river plume input stimulated phytoplankton growth, especially diatoms, resulting in higher relative contribution of phytoplankton carbon (55%) and diatoms (34%) to POC in the plume-impacted region than those (33% and 13%) in high salinity area, respectively. Phytoplankton carbon (up to 538 µg/L) in the plume-impacted region was much higher than that (<166 µg/L) in high salinity area. Our findings were helpful to improve the biogeochemical model in coastal waters adjacent to the ZRE.

Key words: chlorophyll *a*, particulate organic carbon, biogenic silica, phytoplankton carbon, diatoms

Citation: Yu Xiaoyong, Xu Jie, Long Aimin, Li Ruihuan, Shi Zhen, Li Qian P. 2020. Carbon-to-chlorophyll ratio and carbon content of phytoplankton community at the surface in coastal waters adjacent to the Zhujiang River Estuary during summer. *Acta Oceanologica Sinica*, 39(2): 123–131, doi: 10.1007/s13131-020-1556-6

1 Introduction

Chlorophyll *a* (Chl *a*) is extensively used as a proxy of phytoplankton biomass, since Chl *a* is unique to plants and easily measured. However, the concentrations of pigments in phytoplankton cells vary with light and nutrient supply (Chan, 1980; Neale et al., 1989). It is desirable to characterize phytoplankton biomass in form of organic carbon instead of Chl *a*, in order to compare phytoplankton biomass with the biomass of other plankton such as viruses, bacteria and zooplankton (Buck et al., 1996). Furthermore, carbon content is the only variable to express phytoplankton biomass in the biogeochemical or ecological model. However, particulate organic carbon (POC) cannot be used to characterize phytoplankton biomass because it is not specific to phytoplankton and furthermore phytoplankton may not dominate in POC in terms of carbon content in unproductive regions. However, it is difficult to estimate phytoplankton carbon (PC) in marine environments as there is not an approach to separate phytoplankton carbon and non-phytoplankton carbon. Phytoplankton carbon can be estimated by Chl *a* concentration and the C:Chl *a* ratio of phytoplankton since Chl *a* is routinely measured as a robust parameter of phytoplankton biomass in practice. The C:Chl *a* ratio can be obtained by the linear regression of POC vs. Chl *a* concentrations (Cho and Azam, 1990;

Chang et al., 2003).

The C:Chl *a* ratio varies in a wide range across marine environments because of different environmental conditions (Geider, 1993; Buck et al., 1996; Chang et al., 2003; Vázquez-Domínguez et al., 2013). Hence, it is necessary to study the C:Chl *a* ratio across marine environments, in order to estimate the carbon content of the phytoplankton community. In coastal waters, diatoms are often the dominant species of the phytoplankton community, which contribute up to 75% of primary production (Nelson et al., 1995; Tréguer and De La Rocha, 2013). It was ecologically important to quantify the contribution of diatoms to phytoplankton biomass in coastal waters, to better understand the role of diatoms in carbon export in biological pump.

The coastal waters in the northern South China Sea are subjected to the influence of the Zhujiang River discharge during summer (Xu et al., 2008). The Zhujiang River is the second largest river in China in terms of freshwater discharge, with an annual average freshwater discharge of 1.05×10^4 m³/s (Yin et al., 2000). Around 80% of the river discharge occurs in the wet season (April–September). The river plume improved phytoplankton biomass dramatically in coastal waters (Xu et al., 2008). In the plume-impacted coastal waters, phytoplankton carbon and the C:Chl *a* ratio of phytoplankton has never been quantified, which

Foundation item: The National Natural Science Foundation of China under contract No. 41476137; the project of Qingdao National Laboratory for Marine Science and Technology under contract No. QNLM2016ORP0305.

*Corresponding author, E-mail: xujie@scsio.ac.cn

was of significance to improve a biogeochemical model for the northern South China Sea. In this study, the objectives were to compare the C:Chl *a* ratios of phytoplankton and phytoplankton carbon between the plume-impacted coastal waters and the waters with no influence of the plume during summer, as well as the relative contribution of diatoms to the phytoplankton biomass.

2 Materials and methods

2.1 Study sites

A cruise was conducted in June 14 to 29, 2016 in the Zhujiang River Estuary and its adjacent coastal waters aboard the R/V *Haike 68*. A total of 58 stations were visited and vertical profiles of temperature, salinity and fluorescence were measured with a CTD (Sea-bird) at each station. At twenty stations of which, nutrients, chlorophyll *a* (Chl *a*), particulate organic carbon/nitrogen (POC/N) and biogenic silica (BSi) were collected at the surface (Fig. 1).

2.2 Nutrients, Chl *a*, POC/N and BSi

Water samples for nutrients were filtered through the glass fiber filters (GF/F) and immediately frozen (−20°C) until analyzed. Inorganic nutrient concentrations were measured colorimetrically with a Seal AA3 auto analyzer (Bran-Luebbe, GmbH). The low concentrations of NO₂+NO₃ and soluble PO₄ (orthophosphate) within the euphotic zone were measured by the long-cell method (Li et al., 2008; Li and Hansell, 2008) by incorporating a 50 cm liquid waveguide cell to AA3 with detection limits of 0.02 and 0.01 μmol/L, respectively.

For Chl *a* samples, 250 mL to 1 L seawater was filtered on the glass fiber filters (GF/F) and stored at −20°C immediately until analyzed. Chl *a* samples were sonicated for 20 min and extracted in 90% acetone at 4°C in the dark for 24 h. The samples were determined using a Turner Designs Model 10 Fluorometer after being centrifuged at 4 000 r/min for 10 min (Parsons et al., 1984).

The 250 mL to 1 L seawater for POC and PON samples were filtered onto precombusted (4 h at 460°C) 25 mm Whatman GF/F filters. Filters were dried at 60°C in an oven overnight and POC/N was determined with a CHN analyzer (Elementar, Vario El Cube).

Biogenic silica in suspended matter was determined using alkaline extraction method (Ragueneau et al., 2005). Biogenic silica samples were collected on GE polycarbonate membranes (47-mm in diameter, 1 μm in pore size) *in situ* by filtering 250 mL to 1 L

seawater. The filters were kept at −20°C immediately until analyzed. The filter was extracted using 0.2 mol/L NaOH (4.0 mL, pH 13.3) in polypropylene centrifuge tube (Corning, polypropylene, 15 mL) at 100°C for 40 min. After being cooled down to room temperature, 1.0 mL 1.0 mol/L HCl was added to neutralize the pH. Dissolved silicate [Si]₁ and aluminum [Al]₁ concentrations were determined after the supernatant was centrifuged for 10 min at 2 500 r/min. Subsequently, the filter was rinsed with deionized water for three times and dried at 60°C. The filter was digested again following the above digestion procedure. [Si]₂ and [Al]₂ were determined. (Si:Al)₂ ratio was calculated from [Si]₂/[Al]₂ in the second step.

Dissolved silicate concentrations in the supernatant were determined according to the method described by Grasshoff et al. (1999). The dissolved aluminum concentrations were determined with a fluorescence spectrophotometer following the approach described by Ren et al. (2001). The corrected concentration of biogenic silica [BSi] was obtained using the following equation:

$$[\text{BSi}] = [\text{Si}]_1 - [\text{Al}]_1 \times \frac{[\text{Si}]_2}{[\text{Al}]_2}. \quad (1)$$

2.3 Estimate of the C:Chl *a* ratio, phytoplankton carbon, the relative contribution of phytoplankton to POC, the relative contribution of diatoms to phytoplankton biomass and POC

The average C:Chl *a* ratio of phytoplankton was derived from the slope in the regression of POC vs. Chl *a*. Phytoplankton carbon was calculated by multiplying Chl *a* concentration by the average C:Chl *a* ratio of phytoplankton for each sample. The relative contribution of phytoplankton to POC was obtained by dividing PC by POC.

The average Chl *a*:BSi ratio for diatoms was estimated by the slope in the regression of Chl *a* and BSi. The Chl *a* derived from diatoms was obtained by multiplying BSi concentration by the average Chl *a*:BSi ratio for each sample. The relative contribution of diatoms to phytoplankton was obtained by dividing Chl *a* derived from diatoms by Chl *a*. Similarly, the average C:BSi ratio for diatoms was estimated by the slope in the regression of POC and BSi. The POC derived from diatoms was obtained by multiplying BSi concentration by the average C:BSi ratio for each sample. The relative contribution of diatoms to POC was ob-

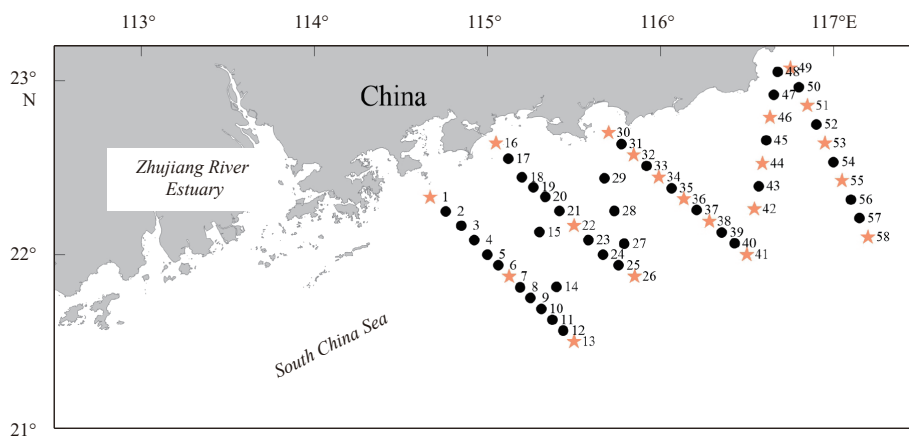


Fig. 1. Location of all sampling stations in coastal waters in the northern South China Sea in June 2016. Circles (●) denote the stations where salinity and temperature were collected. Asterisks (★) represent the stations where salinity, temperature, nutrients, Chl *a*, POC/N and BSi were taken.

tained by dividing POC derived from diatoms by POC.

2.4 Statistical analysis

Statistical analysis was performed using the Origin 8.5 software. A Pearson's test was conducted to determine the significant correlation between variables (salinity, Chl *a*, POC, BSi, PC:POC) ($p < 0.05$).

3 Results

Salinity and temperature exhibited clear spatial variations (Fig. 2). Surface salinity varied in a wide range from 23.5 to 34. High salinity (>33) and low temperature ($<29^{\circ}\text{C}$) were observed in upwelling region near the shore. The plume-impacted region was defined as the area with surface salinity of <32 (Mao et al., 1963). In twenty stations chosen (Table 1), six stations (Stas 13, 16, 30, 46, 49 and 51) with high surface salinity (>32) were considered to be not influenced by the river plume (Fig. 2).

Nutrients, Chl *a*, POC and BSi varied spatially, showing the pattern opposite to salinity. The highest nutrient concentration (NO_3^- : $14.8 \mu\text{mol/L}$, PO_4^{3-} : $0.12 \mu\text{mol/L}$ and SiO_4 : $4.95 \mu\text{mol/L}$) occurred at Sta. 1 with the lowest salinity (23.5) (Table 1). At high salinity (>32) stations, nutrients remained low (NO_3^- : $<0.7 \mu\text{mol/L}$, PO_4^{3-} : $<0.12 \mu\text{mol/L}$, Table 1). Similarly, the concentrations of Chl *a*, POC, PON and BSi were generally high (Chl *a*: 0.92 – $3.79 \mu\text{g/L}$, POC: 21.5 – $67.9 \mu\text{mol/L}$, PON: 2.81 – $13.1 \mu\text{mol/L}$ and BSi: up to $15.0 \mu\text{mol/L}$) at low salinity stations and low (Chl *a*: $<1.30 \mu\text{g/L}$, POC: $<33.0 \mu\text{mol/L}$, PON: $<8.89 \mu\text{mol/L}$ and BSi: mostly $<1.70 \mu\text{mol/L}$) at high salinity stations (Table 1, Fig. 3). C:N ratios (mol/mol) varied from 2.84 to 7.65 at all stations and did not considerably differ between the plume-impacted region and the high

salinity area (Table 1). In addition, there was a significant negative correlation between salinity and these variables (Chl *a*, POC and BSi) (Fig. 4).

A regression between Chl *a*, BSi and POC in the plume-impacted region and high salinity area was observed, respectively (Table 2, Fig. 5). The average ratio of BSi to Chl *a* for diatoms was 0.19 and 0.14 in the plume-impacted region and high salinity area, respectively (Table 2). The relative contribution of diatoms to Chl *a* was on average 51% (14.1%–75.1%) in the plume-impacted region and 29% (11.2%–66.2%) in the high salinity area (Fig. 6, Table 2). The average ratio of BSi to POC was 2.80 and 1.91 in the plume-impacted region and the high salinity area, respectively (Table 2). The relative contribution of diatoms to POC was on average 34% (8.9%–61.8%) in the plume-impacted region and 13% (3.1%–33.6%) in the high salinity area (Fig. 6, Table 2). The average C:Chl *a* ratio (g/g) of phytoplankton was 142 in the plume-impacted region and 135 in the high salinity area, respectively (Table 2). The relative contribution of phytoplankton to POC was 55% (35.0%–72.9%) in the plume-impacted region and 33% (21.5%–48.5%) in the high salinity area (Fig. 6, Table 2). Phytoplankton carbon (PC) varied spatially, with high (up to $538 \mu\text{g/L}$) in the plume-impacted region and low ($<166 \mu\text{g/L}$) in the high salinity area (Fig. 7).

4 Discussion

In summer, a large area of the coastal waters in the northern South China Sea is subjected to the effect of the Zhujiang River Estuary, which delivers huge amount of nutrients. As a result, there was a clear environmental gradient along the inshore-offshore transect, as indicated by spatial variations in salinity. The

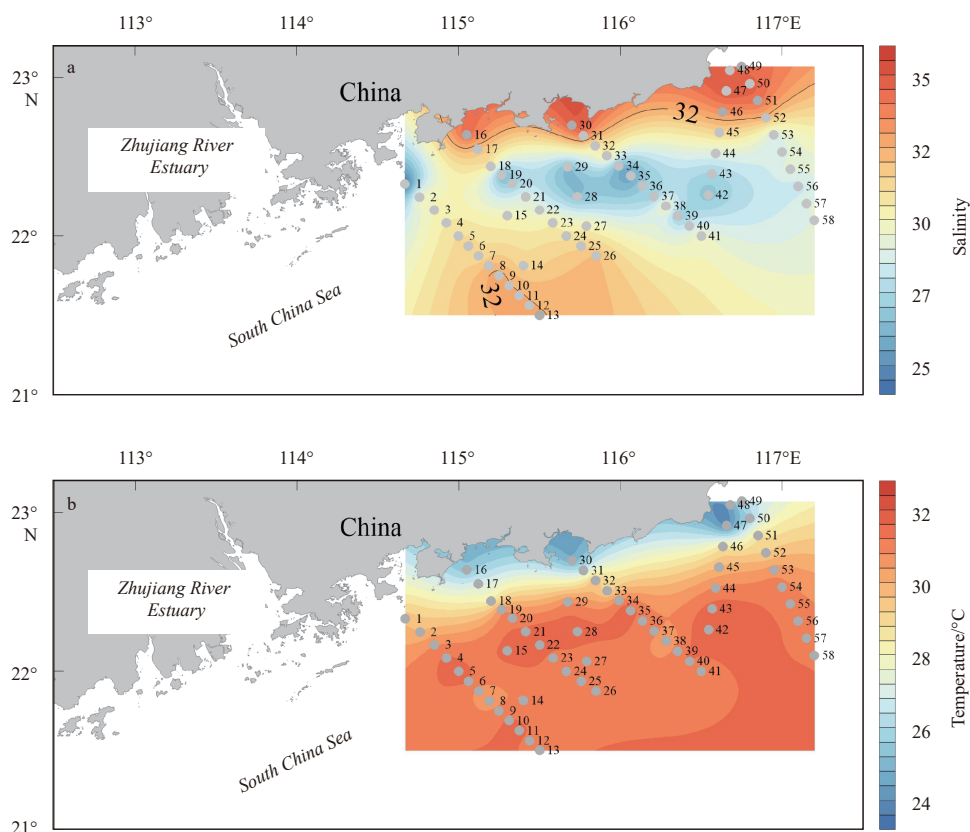
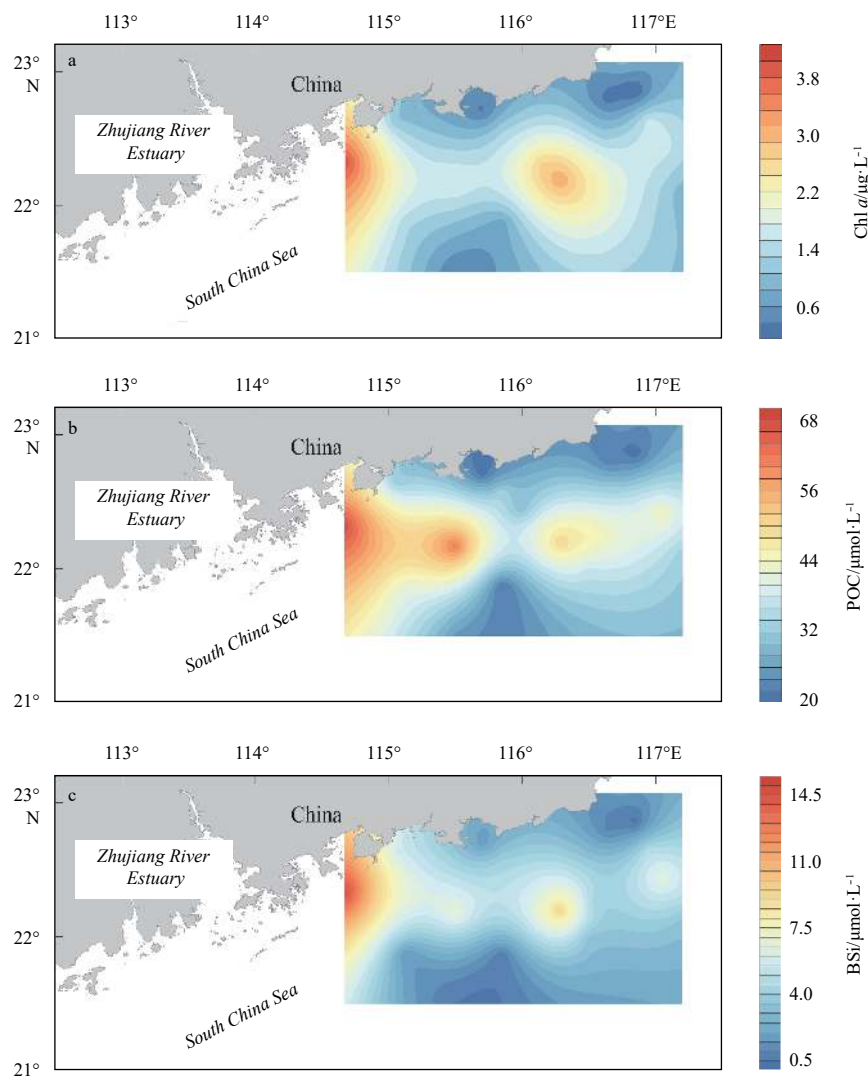


Fig. 2. Changes in temperature (a) and salinity (b) at the surface in coastal waters in the northern South China Sea in June 2016 (●: sampling stations).

Table 1. The concentrations of nutrients, POC, PON and C:N ratios at the surface

| Station | North latitude | East longitude | Nitrate/ $\mu\text{mol}\cdot\text{L}^{-1}$ | Phosphate/ $\mu\text{mol}\cdot\text{L}^{-1}$ | Silicate/ $\mu\text{mol}\cdot\text{L}^{-1}$ | POC/ $\mu\text{mol}\cdot\text{L}^{-1}$ | PON/ $\mu\text{mol}\cdot\text{L}^{-1}$ | C:N ratio |
|---------|----------------|----------------|--|--|---|--|--|-----------|
| 1 | 22.33° | 114.67° | 14.8 | 0.12 | 4.95 | 67.9 | 10.6 | 6.40 |
| 7 | 21.87° | 115.13° | 0.01 | 0.15 | 0.75 | 41.7 | 11.1 | 3.76 |
| 13 | 21.50° | 115.50° | 0.69 | ud | 0.57 | 25.4 | 3.41 | 7.45 |
| 16 | 22.64° | 115.05° | 0.09 | 0.12 | 5.08 | 33.0 | 5.76 | 5.72 |
| 22 | 22.17° | 115.50° | 0.15 | 0.08 | ud | 61.7 | 12.0 | 5.13 |
| 26 | 21.88° | 115.85° | 0.21 | ud | 0.30 | 21.5 | 2.81 | 7.65 |
| 30 | 22.70° | 115.70° | 0.11 | 0.100 | 7.77 | 20.8 | 8.89 | 2.34 |
| 32 | 22.57° | 115.85° | 3.19 | 0.07 | 1.36 | 33.3 | 9.55 | 3.49 |
| 34 | 22.44° | 115.99° | 14.2 | 0.07 | 0.24 | 30.4 | 4.50 | 6.76 |
| 36 | 22.32° | 116.14° | 8.52 | 0.06 | ud | 42.2 | 6.22 | 6.79 |
| 38 | 22.19° | 116.28° | 3.56 | 0.10 | 0.14 | 50.0 | 10.1 | 4.96 |
| 41 | 22.00° | 116.50° | 2.92 | 0.07 | ud | 37.7 | 13.1 | 2.88 |
| 42 | 22.27° | 116.54° | 8.22 | 0.07 | 0.20 | 45.6 | 7.34 | 6.21 |
| 44 | 22.53° | 116.59° | 4.71 | 0.04 | 0.20 | 36.0 | 6.69 | 5.38 |
| 46 | 22.79° | 116.64° | ud | ud | ud | 23.2 | 8.15 | 2.84 |
| 49 | 23.07° | 116.75° | 0.05 | 0.04 | 5.15 | 25.1 | 4.49 | 5.60 |
| 51 | 22.86° | 116.85° | 0.06 | 0.05 | 7.15 | 20.8 | 3.39 | 6.13 |
| 53 | 22.64° | 116.95° | 1.08 | ud | ud | 33.0 | 7.96 | 4.15 |
| 55 | 22.43° | 117.05° | 1.66 | 0.05 | 0.86 | 43.7 | 6.28 | 6.96 |
| 58 | 22.10° | 117.20° | 3.39 | 0.06 | ud | 32.4 | 7.48 | 4.33 |

Note: ud means undetectable.

**Fig. 3.** Chl *a* (a), POC (b) and BSi (c) concentrations at the surface in coastal waters in the northern South China Sea in June 2016.

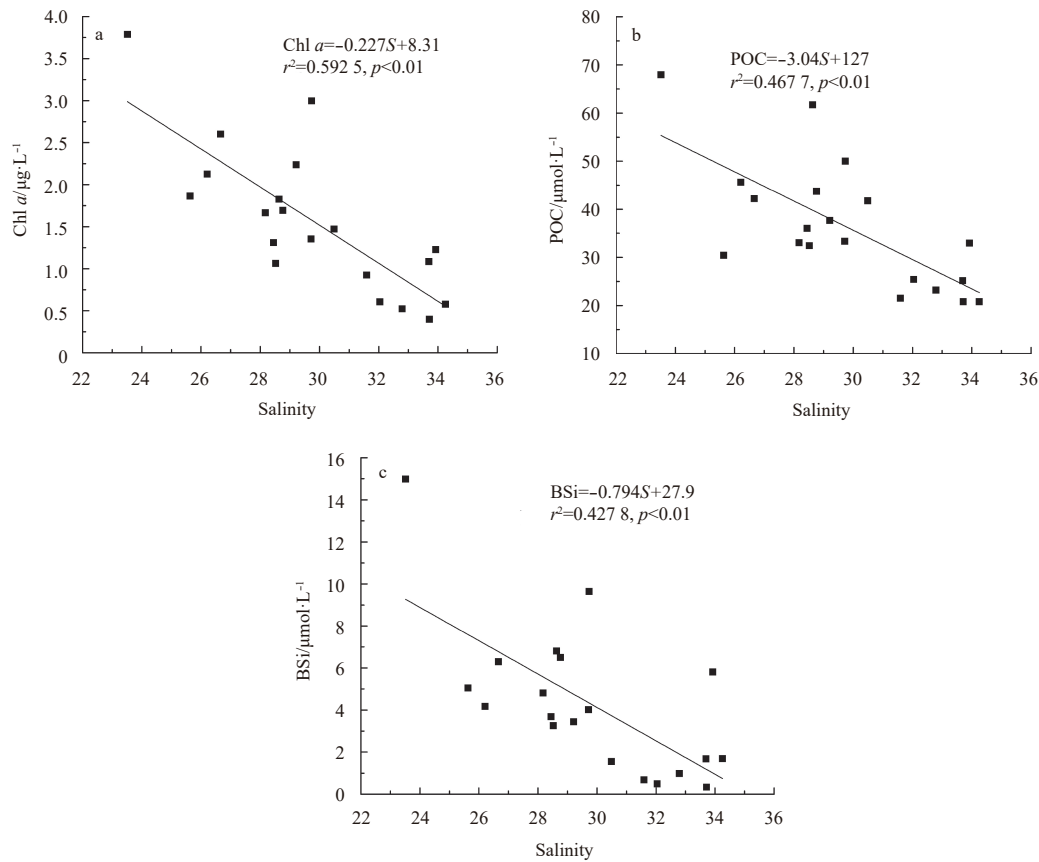


Fig. 4. Correlation analysis between salinity (S) and Chl a (a), POC (b), BSi (c) concentrations at the surface.

Table 2. Correlation analysis between POC, Chl a and BSi concentrations at the surface

| Location | Correlation formula | Correlation coefficient | Average relative contribution |
|-----------------------|---|--------------------------|-------------------------------|
| Plume-impacted region | $\text{POC} = 142 \times \text{Chl } a + 222$ | $r^2 = 0.5266, p < 0.01$ | phytoplankton to POC: 55% |
| High salinity area | $\text{POC} = 135 \times \text{Chl } a + 197$ | $r^2 = 0.6350, p < 0.05$ | phytoplankton to POC: 33% |
| Plume-impacted region | $\text{Chl } a = 0.19 \times \text{BSi} + 0.89$ | $r^2 = 0.7565, p < 0.01$ | diatoms to phytoplankton: 51% |
| High salinity area | $\text{Chl } a = 0.14 \times \text{BSi} + 0.49$ | $r^2 = 0.5832, p < 0.05$ | diatoms to phytoplankton: 29% |
| Plume-impacted region | $\text{POC} = 2.80 \times \text{BSi} + 26.2$ | $r^2 = 0.6278, p < 0.01$ | diatoms to POC: 34% |
| High salinity area | $\text{POC} = 1.91 \times \text{BSi} + 21.2$ | $r^2 = 0.6795, p < 0.05$ | diatoms to POC: 13% |

Zhujiang River discharge input not only increased nutrient concentrations but also altered nutrient structure, leading to potential phosphorus limitation (Xu et al., 2008). Chl a , BSi and POC exhibited the same spatial pattern. Furthermore, salinity was significantly correlated with Chl a , BSi and POC (Fig. 4). These results suggested that riverine nutrient input triggered algal growth. Nutrient enrichment favored diatom blooms, resulting in the dominance of diatoms in the phytoplankton community. In nutrient-rich waters, the predominance of diatoms has been reported (Tréguer and De La Rocha, 2013). In addition, a significant correlation between Chl a and BSi concentrations in the plume-impacted region (Table 2, Fig. 5) was observed, confirming that the riverine nutrient input preferentially stimulated diatom growth. BSi and Chl a are the robust proxy of diatoms and phytoplankton biomass, respectively. According to the relationship between Chl a and BSi, it was estimated that diatoms contributed to on average 51% of Chl a -based phytoplankton biomass in the plume-impacted region, which was higher than that (29%) in the high salinity region. Correspondingly, it was estimated that diatoms made up 34% and 13% of POC in the plume-impacted

region and high salinity area, respectively. Furthermore, the relative contribution of diatoms to POC and Chl a -based phytoplankton biomass was enhanced in the plume-impacted region, corroborating that diatoms outcompeted other phytoplankton groups as nutrients increased. Hence, the riverine nutrient input shifted the phytoplankton community composition and enhanced the contribution of diatoms to primary production.

POC:PON ratio (mol/mol) was on average 5.27 in this study. Meyer et al. (1994) suggested that the C:N ratio was 4–10 for phytoplankton, 6–8 for freshwater algae, approximately 5 for marine algae and more than 20 for terrestrial plants. Hence, POC primarily originated from marine organisms in the study area. In estuarine and coastal waters, POC origins were complicated and resulted from both phytoplankton-derived carbon and non-phytoplankton-derived carbon (Wienke and Cloern, 1987). It was very difficult to separate phytoplankton-derived carbon from non-phytoplankton-derived carbon. However, it was ecologically important to quantify the phytoplankton-derived carbon in aquatic environments. The regression of POC and Chl a is often used to estimate the phytoplankton-derived carbon by the C:Chl

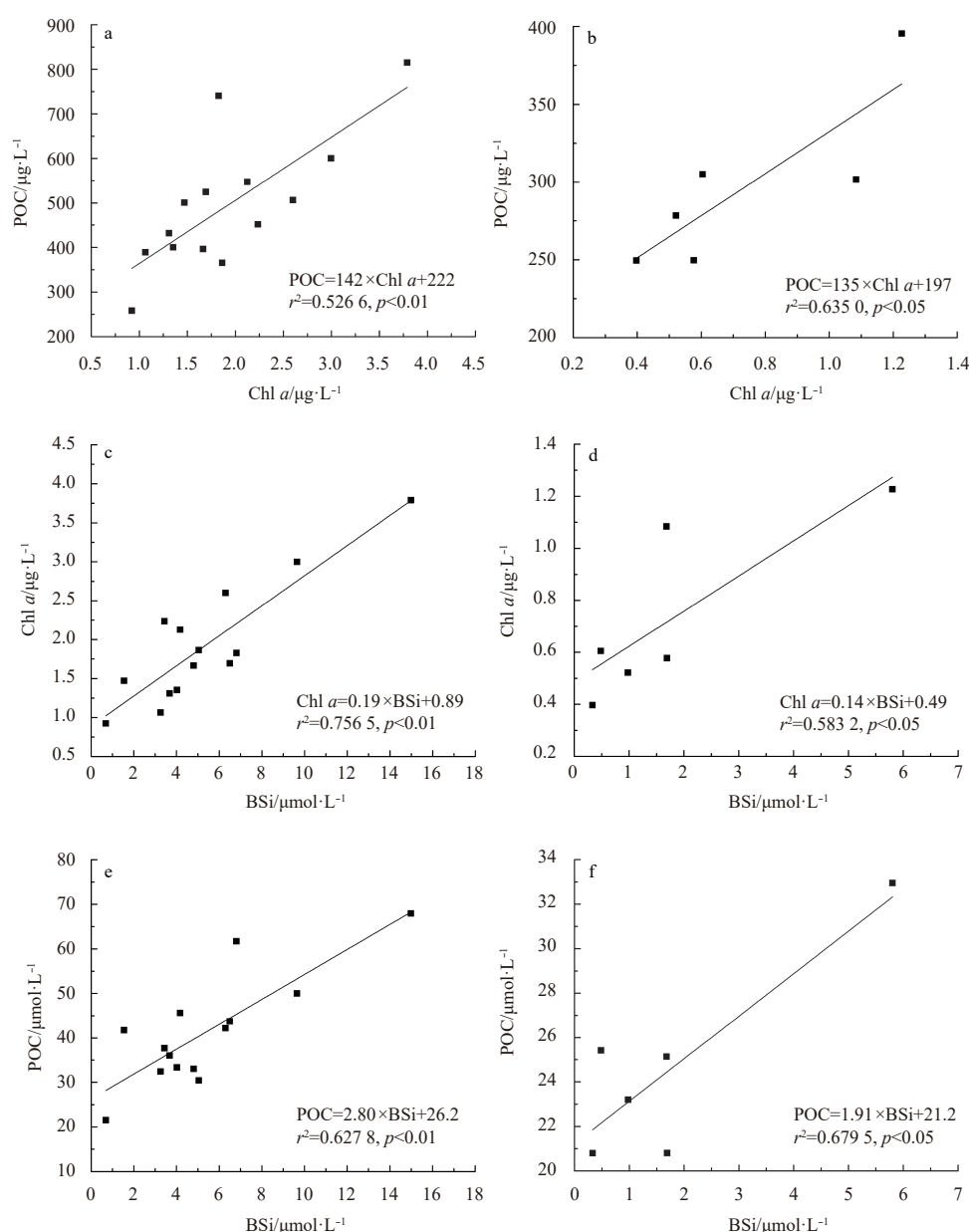


Fig. 5. The correlation analysis between POC and Chl *a* (a, b), Chl *a* and BSi (c, d), and POC and BSi (e, f) concentrations at the surface. a, c and e. Plume-impacted region; and b, d and f. high salinity area.

a ratio (Chang et al., 2003; Jakobsen and Markager, 2016). In our study, the C:Chl *a* ratio of phytoplankton at the surface was on average 142 in the plume-impacted region and 135 in high salinity area with no effect of the river plume, respectively.

The C:Chl *a* ratios of phytoplankton in aquatic environments are generally regulated by numerous factors, such as temperature, light, nutrient concentrations (Zeitzschel, 1970). Laws and Bannister (1980) found that algae were able to adjust cellular carbon and chlorophyll quota according to the light levels. Nutrient limitation is regarded as an important factor for high C:Chl *a* ratio, which induces an increase in the C:Chl *a* ratios of phytoplankton (Hunter and Laws, 1981; Taylor et al., 1997). Generally, C:Chl *a* ratio was low in the light-limited conditions and high in high light levels and low nutrient conditions (Hunter and Laws, 1981; Taylor et al., 1997). The high salinity area was characterized by the pristine seawater with low nutrient concentrations

($\text{NO}_3 < 1 \mu\text{mol/L}$, $\text{PO}_4 < 0.15 \mu\text{mol/L}$; Table 1). In the plume-impacted region, despite of high nutrient input, phosphorus limitation occurred, while nitrogen limitation occurred in regions with no influence of the river plume in the South China Sea (Xu et al., 2008). Phosphorus limitation improved the C:Chl *a* ratios of phytoplankton. Redalje and Laws (1981) found that the C:Chl *a* ratios of phytoplankton increased to 200–300 for diatoms under nutrient-limited conditions. Furthermore, light levels in summer were high at the surface in tropical coastal waters we studied. Hence, high C:Chl *a* ratios of phytoplankton at the surface were attributed to high light intensity and nutrient limitation.

The C:Chl *a* ratios of phytoplankton reported were variable in a wide range across environments, such as 18.0–94.4 in the East China Sea (Chang et al., 2003), (>100) in the Columbia Estuary (Small and Prahl, 2004), (>100) in the surface zone in the North Atlantic Ocean (Buck et al., 1996) and 250 in the Jiaozhou Bay (Lü

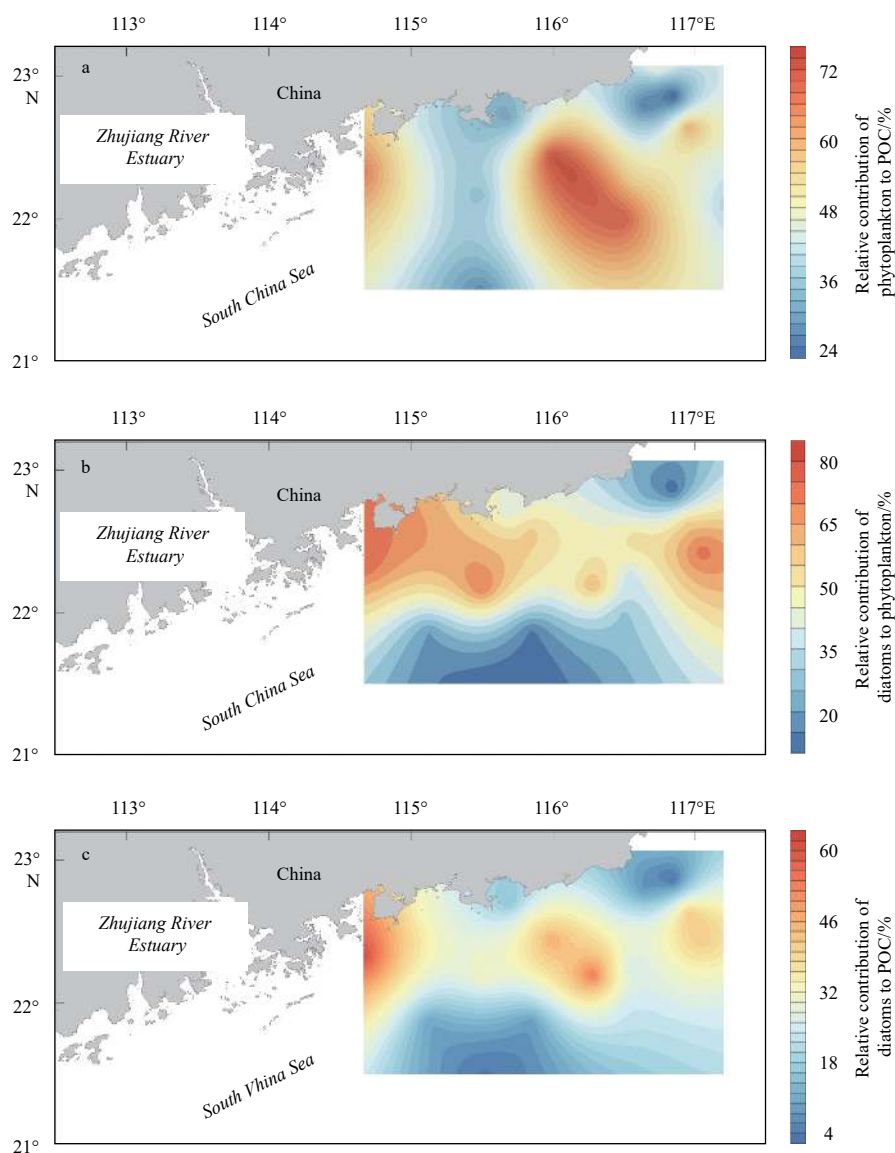


Fig. 6. The relative contribution of phytoplankton to POC (a), diatoms to phytoplankton (b) and diatoms to POC (c) at the surface in coastal waters in June 2016.

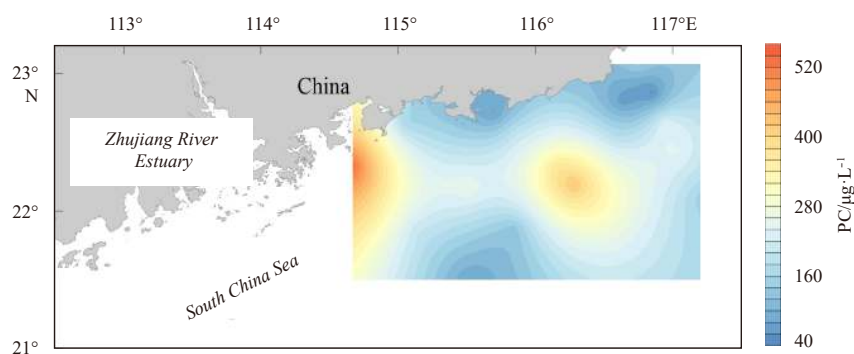


Fig. 7. Phytoplankton carbon concentrations at the surface in coastal waters in the northern South China Sea in June 2016.

et al., 2009). Compared to the C:Chl *a* ratio (94) of phytoplankton in oligotrophic offshore waters of the East China Sea (Chang et al., 2003), the C:Chl *a* ratios of phytoplankton were higher in

coastal waters adjacent to the Zhujiang River Estuary. The study area was located in a tropical region, where light intensity should be higher than that in the East China Sea, which was partly re-

sponsible for higher C:Chl *a* ratio of phytoplankton in pristine high salinity area than offshore waters in the East China Sea.

Based on the C:Chl *a* ratios of phytoplankton, phytoplankton carbon (up to 538 $\mu\text{g/L}$) in the plume-impacted region was higher than that (<166 $\mu\text{g/L}$) in high salinity area. In addition, the fraction of PC to POC was significantly negatively correlated with salinity (Fig. 8). These results suggested that the riverine nutrients stimulated phytoplankton growth and improved the relative contribution of phytoplankton carbon to POC.

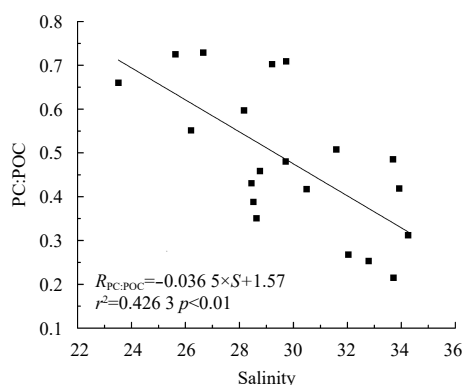


Fig. 8. Correlation analysis between PC:POC ($R_{\text{PC:POC}}$) and salinity at the surface.

5 Conclusions

In summary, the C:Chl *a* ratio of phytoplankton was high in coastal waters adjacent to the ZRE, likely because of high light intensity and nutrient limitation. The Zhujiang River discharge input triggered algal blooms, especially diatom blooms, improved phytoplankton carbon content and its relative contribution to POC. To our knowledge, this was the first time to report the C:Chl *a* ratio of phytoplankton, phytoplankton carbon, the relative contribution of phytoplankton and diatoms to POC in coastal waters influenced by the Zhujiang River discharge. Our findings would be useful to improve the biogeochemical model in the northern South China Sea.

Acknowledgements

We thank Dongxiao Wang for providing the CTD data and Kedong Yin for providing POC/N data.

References

- Buck K R, Chavez F P, Campbell L. 1996. Basin-wide distributions of living carbon components and the inverted trophic pyramid of the central gyre of the North Atlantic Ocean, Summer 1993. *Aquatic Microbial Ecology*, 10(3): 283–298, doi: [10.3354/ame010283](https://doi.org/10.3354/ame010283)
- Chan A T. 1980. Comparative physiological study of marine diatoms and dinoflagellates in relation to irradiance and cell-size. II. Relationship between photosynthesis, growth, and carbon/chlorophyll *a* ratio. *Journal of Phycology*, 16(3): 428–432, doi: [10.1111/j.1529-8817.1980.tb03056.x](https://doi.org/10.1111/j.1529-8817.1980.tb03056.x)
- Chang J, Shiah F K, Gong G C, et al. 2003. Cross-shelf variation in carbon-to-chlorophyll *a* ratios in the East China Sea, Summer 1998. *Deep Sea Research Part II: Topical Studies in Oceanography*, 50(6–7): 1237–1247, doi: [10.1016/S0967-0645\(03\)00020-1](https://doi.org/10.1016/S0967-0645(03)00020-1)
- Cho B C, Azam F. 1990. Biogeochemical significance of bacterial biomass in the ocean's euphotic zone. *Marine Ecology Progress Series*, 63: 253–259, doi: [10.3354/meps063253](https://doi.org/10.3354/meps063253)

- Geider R J. 1993. Quantitative phytoplankton physiology: implications for primary production and phytoplankton growth. In: *Proceedings of ICES Marine Science Symposium*. Vol 197. Oxford: Oxford University Press, 52–62
- Grasshoff K, Kremling K, Ehrhardt M. 1999. *Methods of Seawater Analysis*. 3rd ed. Weinheim: Wiley-VCH, 159–228
- Hunter B L, Laws E A. 1981. ATP and chlorophyll *a* as estimators of phytoplankton carbon biomass. *Limnology and Oceanography*, 26(5): 944–956, doi: [10.4319/lo.1981.26.5.0944](https://doi.org/10.4319/lo.1981.26.5.0944)
- Jakobsen H H, Markager S. 2016. Carbon-to-chlorophyll ratio for phytoplankton in temperate coastal waters: seasonal patterns and relationship to nutrients. *Limnology and Oceanography*, 61(5): 1853–1868, doi: [10.1002/lno.10338](https://doi.org/10.1002/lno.10338)
- Laws E A, Bannister T T. 1980. Nutrient- and light-limited growth of *Thalassiosira fluviatilis* in continuous culture, with implications for phytoplankton growth in the ocean. *Limnology and Oceanography*, 25(3): 457–473, doi: [10.4319/lo.1980.25.3.0457](https://doi.org/10.4319/lo.1980.25.3.0457)
- Li Q P, Hansell D A. 2008. Nutrient distributions in baroclinic eddies of the oligotrophic North Atlantic and inferred impacts on biology. *Deep Sea Research Part II: Topical Studies in Oceanography*, 55(10–13): 1291–1299, doi: [10.1016/j.dsr2.2008.01.009](https://doi.org/10.1016/j.dsr2.2008.01.009)
- Li Q P, Hansell D A, Zhang Jiazhong. 2008. Underway monitoring of nanomolar nitrate plus nitrite and phosphate in oligotrophic seawater. *Limnology and Oceanography: Methods*, 6(7): 319–326, doi: [10.4319/lom.2008.6.319](https://doi.org/10.4319/lom.2008.6.319)
- Lü Shuguo, Wang Xuchen, Han Boping. 2009. A field study on the conversion ratio of phytoplankton biomass carbon to chlorophyll-*a* in Jiaozhou Bay, China. *Chinese Journal of Oceanology and Limnology*, 27(4): 793–805, doi: [10.1007/s00343-009-9221-0](https://doi.org/10.1007/s00343-009-9221-0)
- Mao H L, Kan T C, Lan S F. 1963. A preliminary study of the Yangtze diluted water and its mixing processes. *Oceanologia et Limnologia Sinica (in Chinese)*, 5(3): 183–206
- Meyers P A. 1994. Preservation of elemental and isotopic source identification of sedimentary organic matter. *Chemical Geology*, 114(3–4): 289–302, doi: [10.1016/0009-2541\(94\)90059-0](https://doi.org/10.1016/0009-2541(94)90059-0)
- Neale P J, Cullen J J, Yentsch C M. 1989. Bio-optical inferences from chlorophyll *a* fluorescence: What kind of fluorescence is measured in flow cytometry? *Limnology and Oceanography*, 34(8): 1739–1748, doi: [10.4319/lo.1989.34.8.1739](https://doi.org/10.4319/lo.1989.34.8.1739)
- Nelson D M, Tréguer P, Brzezinski M A, et al. 1995. Production and dissolution of biogenic silica in the ocean: revised global estimates, comparison with regional data and relationship to biogenic sedimentation. *Global Biogeochemical Cycles*, 9(3): 359–372, doi: [10.1029/95GB01070](https://doi.org/10.1029/95GB01070)
- Parsons T R, Maita Y, Lalli C M. 1984. *A Manual of Chemical & Biological Methods for Seawater Analysis*. Oxford: Pergamon Press, 101–104
- Ragueneau O, Savoye N, Del Amo Y, et al. 2005. A new method for the measurement of biogenic silica in suspended matter of coastal waters: using Si: Al ratios to correct for the mineral interference. *Continental Shelf Research*, 25(5–6): 697–710, doi: [10.1016/j.csr.2004.09.017](https://doi.org/10.1016/j.csr.2004.09.017)
- Redalje D G, Laws E A. 1981. A new method for estimating phytoplankton growth rates and carbon biomass. *Marine Biology*, 62(1): 73–79, doi: [10.1007/BF00396953](https://doi.org/10.1007/BF00396953)
- Ren Jingling, Zhang Jing, Luo Jingqing, et al. 2001. Improved fluorimetric determination of dissolved aluminium by micelle-enhanced lumogallion complex in natural waters. *Analyst*, 126(5): 698–702, doi: [10.1039/b007593k](https://doi.org/10.1039/b007593k)
- Small L F, Prahl F G. 2004. A particle conveyor belt process in the Columbia river estuary: evidence from chlorophyll *a* and particulate organic carbon. *Estuaries*, 27(6): 999–1013, doi: [10.1007/BF02803426](https://doi.org/10.1007/BF02803426)
- Taylor A H, Geider R J, Gilbert F J H. 1997. Seasonal and latitudinal dependencies of phytoplankton carbon-to-chlorophyll *a* ratios: results of a modelling study. *Marine Ecology Progress Series*, 152: 51–66, doi: [10.3354/meps152051](https://doi.org/10.3354/meps152051)

- Tréguer P J, De La Rocha C L. 2013. The world ocean silica cycle. *Annual Review of Marine Science*, 5: 477–501, doi: [10.1146/annurev-marine-121211-172346](https://doi.org/10.1146/annurev-marine-121211-172346)
- Vázquez-Domínguez E, Morán X A G, López-Urrutia A. 2013. Photoacclimation of picophytoplankton in the central Cantabrian Sea. *Marine Ecology Progress Series*, 493: 43–56, doi: [10.3354/meps10549](https://doi.org/10.3354/meps10549)
- Wienke S M, Cloern J E. 1987. The phytoplankton component of seston in San Francisco Bay. *Netherlands Journal of Sea Research*, 21(1): 25–33, doi: [10.1016/0077-7579\(87\)90020-2](https://doi.org/10.1016/0077-7579(87)90020-2)
- Xu Jie, Ho A Y T, Yin Kedong, et al. 2008. Temporal and spatial variations in nutrient stoichiometry and regulation of phytoplankton biomass in Hong Kong waters: influence of the Pearl River outflow and sewage inputs. *Marine Pollution Bulletin*, 57(6–12): 335–348, doi: [10.1016/j.marpolbul.2008.01.020](https://doi.org/10.1016/j.marpolbul.2008.01.020)
- Yin Kedong, Qian Peiyuan, Chen J C, et al. 2000. Dynamics of nutrients and phytoplankton biomass in the Pearl River Estuary and adjacent waters of Hong Kong during summer: preliminary evidence for phosphorus and silicon limitation. *Marine Ecology Progress Series*, 194: 295–305, doi: [10.3354/meps194295](https://doi.org/10.3354/meps194295)
- Zeitzschel B. 1970. The quantity, composition and distribution of suspended particulate matter in the Gulf of California. *Marine Biology*, 7(4): 305–318, doi: [10.1007/BF00750823](https://doi.org/10.1007/BF00750823)